AIP Physics of Plasmas

Gyrokinetic theory of fast wave transmission with arbitrary parallel wave number in a nonuniformly magnetized plasma

C. N. LashmoreDavies and R. O. Dendy

Citation: Phys. Fluids B 4, 493 (1992); doi: 10.1063/1.860247
View online: http://dx.doi.org/10.1063/1.860247
View Table of Contents: http://pop.aip.org/resource/1/PFBPEI/v4/i3
Published by the American Institute of Physics.

Gyrokinetic theory of fast wave transmission with arbitrary parallel wave number in a nonuniformly magnetized plasma

C. N. Lashmore-Davies and R. O. Dendy
AEA Fusion, Culham Laboratory (Euratom/UKAEA Fusion Association), Abingdon, Oxfordshire OX14 3DB, England

(Received 13 September 1990; accepted 14 November 1991)

The gyrokinetic theory of ion cyclotron resonance is extended to include propagation at arbitrary angles to a straight equilibrium magnetic field with a linear perpendicular gradient in strength. The case of the compressional Alfvén wave propagating in a $D(^3He)$ plasma is analyzed in detail. A self-consistent local dispersion relation is obtained using a single mode description; this approach enables three-dimensional effects to be included and permits efficient calculation of the transmission coefficient. The dependence of this quantity on the species density ratio, minority temperature, plasma density, magnetic field, and equilibrium scale length is obtained. A self-consistent treatment of the variation of the field polarization across the resonant region is included. Families of transmission curves are given as a function of the normalized parallel wave number for parameters relevant to JET [see, for example, J. Jacquinot *et al.*, Plasma Phys. **30**, 1467 (1988)]. Perpendicular absorption by the minority ions is also discussed, and shown to depend on a single parameter, the ratio of the ion thermal velocity to the Alfvén speed.

I. INTRODUCTION

The variation of an inhomogeneous equilibrium magnetic field across the Larmor orbit of each plasma particle must be included in any fully self-consistent treatment of cyclotron resonance. This requires information about particle gyrophase to be retained at a much later stage in the calculation than in the usual locally uniform approximation. A gyrokinetic approach is therefore required and, recently, the gyrokinetic theory generalized to arbitrary frequencies by Chen and Tsai[1,2] has been applied to cyclotron resonance of a wave propagating perpendicular to a nonuniform equilibrium magnetic field.[3,4] For the case of perpendicular propagation, it was first pointed out in Ref. 5 that gyrokinetic theory enables an additional absorption mechanism or resonance broadening effect to be identified.[3-5] In this paper, we shall extend the previous analysis to the important case where $\mathbf{k}\cdot\mathbf{B}\neq 0$, where $\mathbf{k}$ is the wave vector and $\mathbf{B}$ is the equilibrium magnetic field. The inclusion of the parallel wave number k_z in the present analysis requires two resonance broadening mechanisms to be included simultaneously, since the addition of k_z introduces the familiar Doppler broadening. In order to illustrate the method, we shall concentrate on the specific example of the fast wave propagating in the vicinity of the fundamental minority resonance of a plasma containing two ion species. We assume that the majority species is nonresonant, and in the numerical examples, we consider only the case where the nonresonant species is deuterium and the resonant species helium-3.

Let us consider some of the key parameters in our problem. The first is ρ/L, where ρ is the Larmor radius and L is the scale length of the inhomogeneous equilibrium magnetic field. For tokamak applications, ρ/L is always much smaller than unity. The second parameter is $k_\perp\rho$, where $k_\perp$ is the perpendicular wave number. This parameter may in general be $O(1)$ or greater—it need not be small. A third parameter, specific to the case of a plasma with two ion species, is n_{0b}/n_{0a}, where n_{0a} and n_{0b} are the number densities of the majority and minority ion species, respectively. Again, n_{0b}/n_{0a} is not necessarily small in a tokamak. There have been various approaches to the self-consistent description of cyclotron resonance,[3-10] which differ in their treatment of these parameters. The gyrokinetic approach is specifically designed to include the effect of $k_\perp\rho$ to all orders, while using ρ/L as an expansion parameter, and includes no restriction on n_{0b}/n_{0a}. Its formalism is also sufficiently general to include integral, full wave, or single-mode descriptions.

For the present application, we first derive the self-consistent local dispersion relation to $O(k_\perp^2\rho^2)$. This dispersion relation incorporates the particle response to the perturbed electromagnetic field in a nonuniform equilibrium magnetic field, by taking account of the variation of the equilibrium magnetic field across the Larmor orbits of ions at or near cyclotron resonance. Gyrokinetic theory is at present the only method of treating these problems which includes this effect, and is valid for arbitrary minority to majority density ratios. The self-consistent local dispersion relation contains all the information related to the wave interactions in the resonance region. It contains both the new broadening mechanism and the Doppler effect, as well as the various waves that exist in this frequency range. The self-consistent dispersion relation is the starting point for more accurate theories. For example, for $k_\perp\rho \ll 1$ it has been used to generate the full wave differential equations for the resonance region,[11] and for $k_\perp\rho \gtrsim 1$ it leads to integrodifferential equations. The latter analysis will be presented at a later date.

Since the principal aim of this paper is to investigate the consequences of the inclusion of an additional resonance broadening term due to the inhomogeneity of $\mathbf{B}$, we follow

 0899-8221/92/030493-11$04.00

the simplest approach: a single-mode theory where only the propagation of the fast wave is considered. This provides a rapid and accurate means of calculating the transmission coefficient, provided the minority to majority density ratio is below a critical value derived in Sec. III. For larger values of this ratio, the self-consistent local dispersion relation must be used to generate a full wave theory; this will be the subject of a future publication.

Other approaches to a theory of cyclotron resonance in a nonuniform equilibrium magnetic field include those of Imre *et al.*,[6] who use boundary-layer analysis to obtain full wave equations, and Gambier and Samain,[7] who construct a variational principle that is similar in spirit to gyrokinetic theory but which is aimed specifically at a numerical solution. Romero and Morales[8] obtain a solution to the wave propagation problem in a nonuniform field by means of an expansion in the small parameters (ρ/L), and $k_\perp\rho$. Both the thermal corrections, which depend on $k_\perp\rho$, and the corrections resulting from nonuniformity are contained in this expansion up to $O(k_\perp^2\rho^2)$ and $O(\rho^2/L^2)$. Recall, however, that gyrokinetic theory is specifically designed to include the effects of $k_\perp\rho$ to all orders. Ye and Kaufman[9,10] have also analyzed fast wave heating in the ion cyclotron range of frequencies. They have developed a novel analytic technique for solving the full wave equations, which has been applied to second-harmonic resonance[9] and more recently to minority heating.[10] In Ye and Kaufman's approach, the fast wave is coupled to the resonance by an expansion procedure in which either $k_\perp^2\rho_i^2$ or n_{0b}/n_{0a} is a small expansion parameter, where ρ_i is the ion Larmor radius.

This paper is organized as follows. In Sec. II, we describe the generalization of our gyrokinetic formalism to include arbitrary values of k_z. In Sec. III, we obtain the self-consistent local dispersion relation, valid for any minority to majority density ratio and for any k_z; a perturbation solution is given. We present numerical solutions to the general dispersion relation and further numerical results on the perpendicular absorption mechanism in Sec. IV, and the conclusions are given in Sec. V.

II. GYROKINETIC THEORY OF CYCLOTRON RESONANCE FOR ARBITRARY k_z

We shall begin from the gyrokinetic equation given in Ref. 4 [Eq. (28)]. This is

$$\langle L_g\rangle_l\langle\delta H_g\rangle_l=\frac{iq}{m}\left(\omega\frac{\partial F_{g0}}{\partial\epsilon}+\frac{l\Omega}{B}\frac{\partial F_{g0}}{\partial\mu}\right)\langle\delta\psi_g\rangle_l;\quad(1)$$

here the operator $\langle L_g\rangle_l$ is given by

$$\langle L_g\rangle_l=(\hat{v}_\parallel\mathbf{e}_\parallel+\mathbf{v}_d)\cdot\nabla_X-i(\omega-l\Omega+l\omega_\alpha),\qquad(2)$$

and $\langle\delta\psi_g\rangle_l$, $\langle\delta H_g\rangle_l$ are related to the Fourier transforms in the gyrophase angle of the perturbed electromagnetic field and the perturbed distribution function. For further details and definitions of notation the reader is referred to Ref. 4.

We shall again consider the following simple model of the nonuniform equilibrium magnetic field:

$$\mathbf{B}=\mathbf{e}_zB(1+x/L_B),\qquad(3)$$

where in the simple slab model z is interpreted as the toroidal direction, x as the radial direction, and y as the poloidal direction. The scale length L_B corresponds to the tokamak major radius. In order to obtain a self-consistent local description, we assume all perturbations have a single-mode character given by

$$\delta f(\mathbf{x})=\delta f_\mathbf{k}\exp(i\mathbf{k}\cdot\mathbf{x}),\qquad(4)$$

where

$$\mathbf{k}=k_\perp(\mathbf{e}_x\cos\xi+\mathbf{e}_y\sin\xi)+k_z\mathbf{e}_z.\qquad(5)$$

Combining Eqs. (1), (2), (4), and (5), we obtain the solution of the perturbed gyrokinetic equation,

$$\langle\delta H_g\rangle_l=\frac{(q/m)[\omega(\partial F_{g0}/\partial\epsilon)+(l\Omega/B)(\partial F_{g0}/\partial\mu)]\langle\delta\psi_g\rangle_l}{[k_zv_z+k_yv_d-\omega+l\Omega(X)]}.\qquad(6)$$

Making use of Eq. (4), the quantity $\langle\delta\psi_g\rangle_l$ is obtained as described in Refs. 1–4. The result is

$$\langle\delta\psi_g\rangle_l=e^{i\mathbf{k}\cdot\mathbf{X}}e^{il\xi}\left[J_l\left(\frac{k_\perp v_\perp}{\Omega}\right)\left(\delta\phi_\mathbf{k}+\frac{l\Omega}{k_\perp^2}k_z\frac{\delta A_{\perp\mathbf{k}}}{c}-\frac{v_\parallel}{c}\delta A_{\parallel\mathbf{k}}\right)-\frac{v_\perp}{k_\perp c}J_l'\left(\frac{k_\perp v_\perp}{\Omega}\right)\delta B_{\parallel\mathbf{k}}\right];\qquad(7)$$

here $\mathbf{X}$ denotes the guiding center position, and

$$\delta B_{\parallel\mathbf{k}}=i(k_x\delta A_{y\mathbf{k}}-k_y\delta A_{x\mathbf{k}}).\qquad(8)$$

Equations (6) and (7) are the generalization of the results given in Ref. 4 to the case $k_z\neq0$.

In order to calculate the perturbed currents to substitute into Maxwell's equations, we relate $\langle\delta H_g\rangle_l$ to the total perturbed distribution function in guiding center coordinates and then transform the result into particle coordinates. Following the procedure given in Ref. 4, the perturbed distribution function $\delta f_\mathbf{k}$ expressed as a function of particle coordinates is

$$\delta f_\mathbf{k}=\frac{q}{m}\Bigg((\delta\phi_\mathbf{k}-\langle\delta\psi\rangle_{0\mathbf{k}})\frac{\partial F_0}{\partial\epsilon}+\frac{v_\perp}{c}(\delta A_{x\mathbf{k}}\cos\alpha+\delta A_{y\mathbf{k}}\sin\alpha)\frac{1}{B}\frac{\partial F_0}{\partial\mu}+\sum_{l\neq0}\frac{e^{-il\alpha}[\omega(\partial F_0/\partial\epsilon)+(l\Omega/B)(\partial F_0/\partial\mu)]\langle\delta\psi\rangle_{l\mathbf{k}}}{[k_zv_z+k_yv_d-\omega+l\Omega(x)+(l/L_B)v_\perp\sin\alpha]}\Bigg),\qquad(9)$$

where

$$\langle\delta\psi\rangle_{l\mathbf{k}} = e^{i(k_\perp v_\perp/\Omega)\sin(\alpha-\xi)} e^{il\xi} \times\Bigg[J_l\left(\frac{k_\perp v_\perp}{\Omega}\right)\left(\delta\phi_{\mathbf{k}} + \frac{l\Omega}{k_\perp^2} k_z \frac{\delta A_{\|\mathbf{k}}}{c} - \frac{v_z}{c}\delta A_{\|\mathbf{k}}\right) - \frac{v_\perp}{k_\perp c} J_l'\left(\frac{k_\perp v_\perp}{\Omega}\right)\delta B_{\|\mathbf{k}}\Bigg]. \tag{10}$$

As in Ref. 4, we find it convenient to transform Eqs. (9) and (10) to Cartesian velocity coordinates. Introducing a dimensionless velocity $\mathbf{V} = \mathbf{v}/v_T = (V_\perp \cos\alpha, V_\perp \sin\alpha, V_z)$ where $V_\perp = v_\perp/v_T$ and $V_z = v_z/v_T$, and restricting the analysis to the case of a Maxwellian equilibrium velocity distribution,

$$F_0 = \frac{n_0}{\pi^{3/2} v_T^3}\exp\left(\frac{-v^2}{v_T^2}\right) = \left(\frac{n_0}{\pi^{3/2} v_T^3}\right)\exp\left(\frac{-2\epsilon}{v_T^2}\right), \tag{11}$$

the perturbed distribution function, Eq. (9) becomes

$$\delta f_{\mathbf{k}} = -\frac{2n_0 q}{m v_T^2}\frac{1}{\pi^{3/2} v_T^3} e^{-V_z^2} e^{-V_x^2} e^{-V_y^2}\Bigg\{\delta\phi_{\mathbf{k}} - \langle\delta\psi\rangle_{0\mathbf{k}} + \sum_{l\neq 0}\omega e^{-il\alpha}\langle\delta\psi\rangle_{l\mathbf{k}}\Bigg[k_z v_T\Bigg(V_z + \frac{k_y}{k_z}\frac{v_d}{v_T} - \frac{[\omega - l\Omega(x)]}{k_z v_T} + \frac{l}{k_z L_B} V_y\Bigg)\Bigg]^{-1}\Bigg\}. \tag{12}$$

Similarly, Eq. (10) becomes

$$\langle\delta\psi\rangle_{l\mathbf{k}} = e^{ik_x\rho V_y} e^{-ik_y\rho V_x} e^{il\xi}\Bigg[J_l\left(\frac{k_\perp v_\perp}{\Omega}\right) \times\left(\delta\phi_{\mathbf{k}} + \frac{l\Omega}{k_\perp^2}k_z\frac{\delta A_{\|\mathbf{k}}}{c} - \frac{v_z}{c}\delta A_{\|\mathbf{k}}\right) - \frac{v_\perp}{k_\perp c}J_l'\left(\frac{k_\perp v_\perp}{\Omega}\right)\delta B_{\|\mathbf{k}}\Bigg], \tag{13}$$

where $\rho = v_T/\Omega$.

We may now use Eq. (12) to calculate the perturbed current density. In order to carry out the required velocity integrations we must deal with the resonant denominator. This contains three resonance broadening terms. We have previously noted[3,4] that we may neglect the term $k_y v_d$ due to the equilibrium drift in the magnetic field gradient provided $k_\perp \rho \ll 1$. Since we shall again make this assumption, we reduce the resonance broadening terms to two. However, both these terms depend linearly on a velocity coordinate, so that we may rotate to new velocity coordinates such that the resonance depends only on a single velocity variable. Defining

$$W_y = \tau(V_y - \nu V_z), \tag{14}$$

$$W_z = \tau(\nu V_y + V_z), \tag{15}$$

where

$$\nu = l/k_z L_B \tag{16}$$

and

$$\tau = (1+\nu^2)^{-1/2}, \tag{17}$$

we obtain $dV_y\, dV_z = dW_y\, dW_z$.

We may now calculate the perturbed current

$$\delta\mathbf{J}_{\mathbf{k}} = q v_T^4 \int \delta f_{\mathbf{k}} \mathbf{V}\, dV_x\, dV_y\, dV_z. \tag{18}$$

Since the parallel electric field $\delta E_{z\mathbf{k}} \sim O(m_e/m_i)$ for the compressional Alfvén wave in the ion cyclotron range of frequencies,[12] we need only calculate $\delta J_{x\mathbf{k}}$ and $\delta J_{y\mathbf{k}}$. In order to calculate the resonant current, we make use of the result[4]

$$e^{-il(\alpha-\xi)} = [(k_x \pm ik_y)(V_x \mp iV_y)/k_\perp V_\perp]^{|l|}, \tag{19}$$

where the upper sign refers to $l>0$ and the lower sign to $l<0$. Substituting Eqs. (12), (13), and (19) into Eq. (18), using Eqs. (14)–(17) and expanding the Bessel functions for small argument, the x- and y-components of the current density for the fundamental resonance, $l=1$, are as follows:

$$(\delta J_{x\mathbf{k}})_R = \frac{\omega_{pb}^2}{8\pi}\frac{\omega}{\Omega_b}\frac{k_\perp}{k_z}\frac{\tau}{v_{Tb}} e^{k_\perp^2\rho_b^2/4} \times\Bigg\{\Bigg[ik_y\rho_b\left(a_0 - \frac{i\nu\tau a_q}{2}\right) - a_x\Bigg]Z(\eta_{1b}) + (a_q + ik_y\rho_b a_z - k_y\rho_b\nu\tau a_q\eta_{1b})[1+\eta_{1b}Z(\eta_{1b})]\Bigg\}, \tag{20}$$

$$(\delta J_{y\mathbf{k}})_R = -\frac{\omega_{pb}^2}{8\pi}\frac{\omega}{\Omega_b}\frac{k_\perp}{k_z}\frac{\tau}{v_{Tb}} e^{-k_\perp^2\rho_b^2/4}\Bigg\{i\nu^2\tau^2 a_q + \Bigg[ik_x\rho_b\left(a_0 - \frac{i\nu\tau a_q}{2}\right) + \tau a_y\Bigg]Z(\eta_{1b}) + \Bigg[2\nu\tau a_0 + ik_x\rho_b a_z + i\tau^2(1-2\nu^2)a_q + \nu\tau(2a_z - k_x\rho_b a_q)\eta_{1b} + 2i\nu^2\tau^2 a_q\eta_{1b}^2\Bigg][1+\eta_{1b}Z(\eta_{1b})]\Bigg\}. \tag{21}$$

Here the subscript R represents a contribution from the resonant ions denoted by a subscript b, and the quantity η_{1b} is given by

$$\eta_{1b} = \tau\{[\omega - \Omega_b(x)]/k_z v_T - ik_x\rho_b\nu/2\}. \tag{22}$$

The quantities a_0, a_x, a_y, a_z, and a_q that occur in Eqs. (20) and (21) are given by

$$a_0 = \frac{k_\perp\rho_b}{2}\left(\delta\phi_{\mathbf{k}} + \frac{l\Omega}{k_\perp^2}k_z\frac{\delta A_{\|\mathbf{k}}}{c} - \frac{\Omega}{k_\perp^2}\frac{\delta B_{\|\mathbf{k}}}{c}\right), \tag{23}$$

$$a_x = \frac{(k_x + ik_y)}{k_\perp}\left(\delta\phi_{\mathbf{k}} + \frac{l\Omega}{k_\perp^2}k_z\frac{\delta A_{\|\mathbf{k}}}{c} - \frac{\Omega}{k_\perp^2}\frac{\delta B_{\|\mathbf{k}}}{c}\right), \tag{24}$$

$$a_y = (\nu k_\perp \rho_b \tau v_{Tb}/2c)\delta A_{\parallel \mathbf{k}} - i\tau a_x, \tag{25}$$

$$a_z = -[(k_\perp \rho_b \tau v_{Tb}/2c)\delta A_{\parallel \mathbf{k}} + i\nu\tau a_x], \tag{26}$$

$$a_q = (\tau v_{Tb}/c)[(k_x + ik_y)/k_\perp]\delta A_{\parallel \mathbf{k}}. \tag{27}$$

In the limit $k_z \to 0$, Eqs. (20) and (21) reduce to the expressions for the $l = 1$, resonant perpendicular currents given by Eqs. (60) and (61) in Ref. 4.

We shall now write the resonant current in terms of the perturbed electric field. This will enable us to obtain the electric field polarizations $(\delta E_{x\mathbf{k}} \pm i\delta E_{y\mathbf{k}})/|\delta \mathbf{E}_\perp|$ which are relevant to absorption; it also facilitates comparison with other theories which use the dielectric tensor. Since we shall neglect $\delta E_{z\mathbf{k}}$, we need only consider the following combination of potentials:

$$\delta\phi_\mathbf{k} + (\Omega/k_\perp^2)(k_z \delta A_{\parallel \mathbf{k}}/c) - (\Omega/k_\perp^2)(\delta B_{\parallel \mathbf{k}}/c),$$

where we have now put $l = 1$. Using Eq. (8) and the Coulomb gauge, and putting $\omega = \Omega$, we obtain

$$\delta\phi_\mathbf{k} + \frac{\Omega}{k_\perp^2} k_z \frac{\delta A_{\parallel \mathbf{k}}}{c} - \frac{\Omega}{k_\perp^2} \frac{\delta B_{\parallel \mathbf{k}}}{c} = i \frac{(k_x - ik_y)}{k_\perp^2} (\delta E_{x\mathbf{k}} + i\delta E_{y\mathbf{k}}). \tag{28}$$

We can now write Eqs. (20) and (21) in terms of $\delta E_{x\mathbf{k}}$ and $\delta E_{y\mathbf{k}}$, neglecting the term proportional to $\delta E_{z\mathbf{k}}$, giving

$$(\delta J_{x\mathbf{k}})_R \simeq -\frac{i\tau}{k_z v_{Tb}} \frac{\omega_{pb}^2}{8\pi} e^{-k_\perp^2 \rho_b^2/4} \left[\left(1 - \frac{ik_y \rho_b}{2} (k_x \rho_b - ik_y \rho_b) \right) Z(\eta_{1b}) - \nu\tau k_y \rho_b [1 + \eta_{1b} Z(\eta_{1b})] \right] \times (\delta E_{x\mathbf{k}} + i\delta E_{y\mathbf{k}}), \tag{29}$$

$$(\delta J_{y\mathbf{k}}) \simeq \frac{-\tau^3}{k_z v_{Tb}} \frac{\omega_{pb}^2}{8\pi} e^{-k_\perp^2 \rho_b^2/4} \times \left[\left(1 - \frac{k_x \rho_b}{2\tau} \frac{(k_x \rho_b - ik_y \rho_b)}{\tau} \right) Z(\eta_{1b}) + i\nu \left(\frac{(2k_x \rho_b - ik_y \rho_b)}{\tau} - 2i\nu\eta_{1b} \right) \times [1 + \eta_{1b} Z(\eta_{1b})] \right] (\delta E_{x\mathbf{k}} + i\delta E_{y\mathbf{k}}). \tag{30}$$

Next, we use Eqs. (29) and (30) to obtain the resonant components of the conductivity tensor $(\sigma_{ij})_R$, where i and j represent either x or y:

$$(\sigma_{xx})_R = iQK_1, \tag{31}$$

$$(\sigma_{xy})_R = -QK_1, \tag{32}$$

$$(\sigma_{yx})_R = \tau^2 QK_2, \tag{33}$$

$$(\sigma_{yy})_R = i\tau^2 QK_2, \tag{34}$$

where

$$Q = -(\tau/k_z v_{Tb})(\omega_{pb}^2/8\pi) e^{-k_\perp^2 \rho_b^2/4}, \tag{35}$$

$$K_1 = [1 - (ik_y \rho_b/2)(k_x \rho_b - ik_y \rho_b)] Z(\eta_{1b}) - \nu\tau k_y \rho_b [1 + \eta_{1b} Z(\eta_{1b})], \tag{36}$$

$$K_2 = \left[1 - \frac{k_x \rho_b}{2\tau} \frac{(k_x \rho_b - ik_y \rho_b)}{\tau} \right] Z(\eta_{1b}) + i\nu \left[\frac{(2k_x \rho_b - ik_y \rho_b)}{\tau} - 2i\nu\eta_{1b} \right] \times [1 + \eta_{1b} Z(\eta_{1b})]. \tag{37}$$

We now write

$$\sigma = \sigma_{NR} + \sigma_R, \tag{38}$$

where σ_R is given by Eqs. (31)–(34) and the nonresonant conductivity σ_{NR} is due to the majority ions, denoted by a subscript a, the nonresonant contribution of the minority ions, and the electrons. In order to obtain expressions for the elements of σ_{NR}, it is sufficient to use the conductivity tensor for a uniform plasma, since we only aim to describe the change of the fast wave in the vicinity of the minority resonance. With the aid of Krall and Trivelpiece,[13] we may therefore write

$$(\sigma_{xx})_{NR} \simeq \frac{i}{4\pi} \frac{\omega_{pa}^2}{\Omega_a} \left(\frac{r_1}{(r_1^2 - 1)} - \frac{r_2}{4} \right), \tag{39}$$

$$(\sigma_{xy})_{NR} \simeq -\frac{1}{4\pi} \frac{\omega_{pa}^2}{\Omega_a} \left(\frac{r_1^2}{(r_1^2 - 1)} + \frac{5}{4} r_2 \right), \tag{40}$$

$$(\sigma_{yx})_{NR} = -(\sigma_{xy})_{NR}, \tag{41}$$

$$(\sigma_{yy})_{NR} = (\sigma_{xx})_{NR}, \tag{42}$$

where $r_1 = \Omega_b/\Omega_a$ and $r_2 = n_{0b} Z_b / n_{0a} Z_a$. We have now assembled all the information required in order to obtain the self-consistent local dispersion relation that will be derived in the next section.

III. THE SELF-CONSISTENT LOCAL DISPERSION RELATION

In order to obtain the local dispersion relation, we combine Maxwell's two curl equations giving

$$\{[k^2 - (\omega^2/c^2)]\mathbf{I} - \mathbf{kk} - (4\pi i\omega/c^2)\boldsymbol{\sigma}\} \cdot \delta \mathbf{E}_\mathbf{k} = 0. \tag{43}$$

Since we neglect $\delta E_{z\mathbf{k}}$, we may write Eq. (43) as a pair of equations:

$$\left(k_y^2 + k_z^2 - \frac{\omega^2}{c^2} - \frac{4\pi i\omega}{c^2} \sigma_{xx} \right) \delta E_{x\mathbf{k}} - \left(k_x k_y + \frac{4\pi i\omega}{c^2} \sigma_{xy} \right) \delta E_{y\mathbf{k}} = 0, \tag{44}$$

$$-\left(k_x k_y + \frac{4\pi i\omega}{c^2} \sigma_{yx} \right) \delta E_{x\mathbf{k}} + \left(k_x^2 + k_z^2 - \frac{\omega^2}{c^2} - \frac{4\pi i\omega}{c^2} \sigma_{yy} \right) \delta E_{y\mathbf{k}} = 0. \tag{45}$$

Using Eqs. (31)–(34) and Eq. (38), and taking the determinant of Eqs. (44) and (45), we obtain the dispersion relation

$$\left(k_z^2-\frac{\omega^2}{c^2}\right)^2+(k_x^2+k_y^2)\left(k_z^2-\frac{\omega^2}{c^2}\right)-\frac{4\pi i\omega}{c^2}(\sigma_{xx})_{NR}\left[2\left(k_z^2-\frac{\omega^2}{c^2}\right)+k_x^2+k_y^2\right]$$
$$-\left(\frac{4\pi\omega}{c^2}\right)^2[(\sigma_{xx})_{NR}^2+(\sigma_{xy})_{NR}^2]-\frac{4\pi i\omega}{c^2}\left[iQK_1\left(k_x^2+k_z^2-\frac{\omega^2}{c^2}\right)\right.$$
$$\left.+i\tau^2QK_2\left(k_y^2+k_z^2-\frac{\omega^2}{c^2}\right)+k_xk_yQ(\tau^2K_2-K_1)\right]-\left(\frac{4\pi\omega}{c^2}\right)^2Q(\tau^2K_2+K_1)[i(\sigma_{xx})_{NR}-(\sigma_{xy})_{NR}]=0. \quad (46)$$

Substituting Eqs. (39)–(42) into Eq. (46), the dispersion relation becomes

$$\frac{\omega_{pa}^2}{\Omega_a^2}\frac{\omega^2}{c^2}\frac{\Omega_a}{\omega}\frac{r_1}{(r_1^2-1)}\left\{\left[\left[1-\frac{r_2}{4}\frac{(r_1^2-1)}{r_1}+\frac{\Omega_a^2}{\omega_{pa}^2}\frac{c^2}{\omega^2}\frac{\omega}{\Omega_a}\frac{(r_1^2-1)}{r_1}\left(k_z^2-\frac{\omega^2}{c^2}\right)\right]k_\perp^2\right.\right.$$
$$-\frac{\omega_{pa}^2}{c^2}\frac{\omega}{\Omega_a}r_1\left[1+\frac{r_2}{2}\left(1+5r_1+3r_2\frac{(r_1^2-1)}{r_1}\right)\right]+2\left(1-\frac{r_2}{4}\frac{(r_1^2-1)}{r_1}\right)\left(k_z^2-\frac{\omega^2}{c^2}\right)$$
$$\left.+\frac{\Omega_a^2}{\omega_{pa}^2}\frac{c^2}{\omega^2}\frac{\omega}{\Omega_a}\frac{(r_1^2-1)}{r_1}\left(k_z^2-\frac{\omega^2}{c^2}\right)^2\right]\right\}+4\pi\frac{\omega}{c^2}Q\{(k_x+ik_y)(k_xK_1-ik_y\tau^2K_2)$$
$$\left.-\left[\frac{\omega_{pa}^2}{c^2}\frac{\omega}{\Omega_a}\left(\frac{r_1}{(r_1+1)}+\frac{3r_2}{2}\right)+\frac{\omega^2}{c^2}-k_z^2\right\}(K_1+\tau^2K_2)\right]=0. \quad (47)$$

This is the self-consistent local dispersion relation in three dimensions for the fast wave in the vicinity of the fundamental resonance of one of the ion species in a two-ion-species plasma, where the wave propagates at an arbitrary angle to the magnetic field. The equation must be solved for k_x, since x is the direction of nonuniformity. Putting $k_z=0$, Eq. (47) reduces to the dispersion relation previously derived.[4]

Before discussing the general solution of Eq. (47), we shall obtain a perturbation solution. For this we will allow k_z to remain arbitrary but assume small minority to majority density ratios. The perturbation parameter will therefore be r_2; thus, we neglect r_2 in the nonresonant terms. Substituting Eq. (35) for Q into Eq. (47) we obtain, after a little algebra,

$$N_\perp^2\left[1+(r_1^2-1)\left(N_z^2-\frac{c_A^2}{c^2}\right)\right]-1+2\left(N_z^2-\frac{c_A^2}{c^2}\right)+(r_1^2-1)\left(N_z^2-\frac{c_A^2}{c^2}\right)^2$$
$$=\frac{r_2(r_1^2-1)}{2(k_z^2L_B^2+1)^{1/2}}\frac{\Omega_aL_B}{v_{Tb}}\left[(N_x+iN_y)(N_xK_1-iN_y\tau^2K_2)-\left(\frac{1}{(r_1+1)}+\frac{c_A^2}{c^2}-N_z^2\right)(K_1+\tau^2K_2)\right], \quad (48)$$

where $\mathbf{N}=c_A\mathbf{k}/\omega$ and $N_\perp^2=N_x^2+N_y^2$. We now specialize a little further by setting $N_y=0$ in the interests of simplicity. Substituting for K_1 and K_2 from Eqs. (36) and (37), and neglecting c_A^2/c^2 and terms proportional to v_{Tb}^2/c_A^2, Eq. (48) can be written

$$N_\perp^2-\frac{[1-2N_z^2-(r_1^2-1)N_z^4]}{1+N_z^2(r_1^2-1)}=\frac{r_2(r_1-1)}{2(k_z^2L_B^2+1)^{1/2}}\frac{\Omega_aL_B}{v_{Tb}[1+N_z^2(r_1^2-1)]}$$
$$\times(\{(r_1+1)N_\perp^2-[1-N_z^2(r_1+1)](1+\tau^2)\}Z(\eta_{1b})$$
$$-[1-N_z^2(r_1+1)]2\nu\tau(\nu\tau\eta_{1b}+ik_x\rho_b)[1+\eta_{1b}Z(\eta_{1b})]). \quad (49)$$

We now solve Eq. (49) perturbatively, assuming

$$N_\perp=N_{\perp0}+\delta N_\perp, \quad (50)$$

where

$$N_{\perp0}^2=[1-2N_z^2-(r_1^2-1)N_z^4]/[1+N_z^2(r_1^2-1)]. \quad (51)$$

Substituting Eq. (50) into Eq. (49) we obtain

$$2N_{\perp0}\delta N_\perp\simeq\frac{r_2(r_1-1)}{2(k_z^2L_B^2+1)^{1/2}}\frac{\Omega_aL_B}{v_{Tb}[1+N_z^2(r_1^2-1)]}(\{(r_1+1)[N_{\perp0}^2+(1+\tau^2)N_z^2]-1-\tau^2\}Z(\eta_{1b})$$
$$-2\nu\tau[1-(r_1+1)N_z^2](\nu\tau\eta_{1b}+ik_x\rho_b)[1+\eta_{1b}Z(\eta_{1b})]). \quad (52)$$

We now define

$$p_1=1/(k_z^2L_B^2+1)^{1/2}, \quad (53)$$

$$\zeta_{1b}=(L_B/v_{Tb})[\omega-\Omega_b(x)]. \quad (54)$$

Substituting Eqs. (53) and (54) into Eq. (22) and using Eqs. (16) and (17) we obtain

$$\eta_{1b}=p_1[\zeta_{1b}-i(k_x\rho_b/2)]. \quad (55)$$

We now use the relation

$$Z'(x) = -2[1 + xZ(x)], \tag{56}$$

and assuming $k_x\rho_b \ll \zeta_{1b}$ we obtain

$$Z(\eta_{1b}) \simeq Z(p_1\zeta_{1b}) + ik_x\rho_b p_1[1 + p_1\zeta_{1b}Z(p_1\zeta_{1b})]. \tag{57}$$

Similarly,

$$1 + \eta_{1b}Z(\eta_{1b}) \simeq (1 + ik_x\rho_b p_1)[1 + p_1\zeta_{1b}Z(p_1\zeta_{1b})] - i(k_x\rho_b/2)p_1Z(p_1\zeta_{1b}). \tag{58}$$

Substituting Eqs. (57) and (58) into Eq. (52), we obtain, after further algebra

$$2N_{10}\,\mathrm{Im}\,\delta N_\perp \simeq \frac{p_1 r_2(r_1-1)\Omega_a L_B}{2v_{Tb}[1+N_z^2(r_1^2-1)]}\Bigg(Z_i(p_1\zeta_{1b})\Big\{(r_1+1)[N_{10}^2+(1+\tau^2)N_z^2]-1-\tau^2-2p_1^2[1-(r_1+1)N_z^2]$$
$$\times\left[p_1^2\zeta_{1b}^2+\frac{N_{10}^2v_{Tb}^2}{2c_A^2}\left(1-\frac{p_1^2}{2}\right)(1-2p_1\zeta_{1b})\right]\Big\}+Z_r(p_1\zeta_{1b})N_{10}\frac{v_{Tb}}{c_A}p_1\zeta_{1b}(p_1\{(r_1+1)$$
$$\times[N_{10}^2+(1+\tau^2)N_z^2]-1-\tau^2\}-2p_1[1-(r_1+1)N_z^2](1-p_1^2+p_1^3\zeta_{1b}))+N_{10}\frac{v_{Tb}}{c_A}$$
$$\times\left[p_1\{(r_1+1)[N_{10}^2+(1+\tau^2)N_z^2]-1-\tau^2\}-2p_1\left(1-\frac{p_1^2}{2}+p_1^3\zeta_{1b}\right)[1-(r_1+1)N_z^2]\right]\Bigg). \tag{59}$$

We have previously shown[3,4] that only the part of $\mathrm{Im}\,\delta N_\perp$ which is proportional to Z_i contributes to the optical depth, since only these terms involve the resonant particles. The remaining terms arise from the kinetic power flow and do not produce any net effect on the total absorption, although they can influence the absorption profile. Recalling that the optical depth τ_b is given by

$$\tau_b = 2\int_{-\infty}^{\infty}\mathrm{Im}\,\delta k_\perp(x)dx, \tag{60}$$

using Eqs. (3) and (54) and integrating only the terms in Eq. (59) proportional to Z_i, we obtain

$$\tau_b = \frac{\pi}{2}\frac{\Omega_a L_B}{c_A}\frac{r_2(r_1-1)}{N_{10}[1+N_z^2(r_1^2-1)]}\times\{(r_1+1)[N_z^2(1+\tau^2+p_1^2)+N_{10}^2]-(1+\tau^2+p_1^2)\}; \tag{61}$$

here we have neglected a term proportional to $N_{10}^2v_{Tb}^2/c_A^2 \equiv k_{x0}^2\rho_b^2 \ll 1$. Let us define the quantity

$$\tau_{b\perp} = \frac{\pi}{2}\frac{\Omega_b L_B}{c_A}\frac{r_2}{r_1}(r_1-1)^2. \tag{62}$$

Substituting Eqs. (16), (17), (51), and (53) into Eq. (61) and making use of Eq. (62), the optical depth for oblique propagation can be written

$$\tau_b = \frac{\tau_{b\perp}[1-(r_1+1)N_z^2]^{3/2}}{[1+(r_1^2-1)N_z^2]^{3/2}[1+(r_1-1)N_z^2]^{1/2}}. \tag{63}$$

For $N_z=0$, Eq. (63) reduces to our previous[3,4] result for perpendicular propagation. We may compare Eq. (63) with Francis *et al.*[14] who considered a D(H) plasma. In this case $r_1=2$ and Eq. (63) reduces to

$$\tau_b[\mathrm{D(H)}] = \frac{\pi}{2}\frac{\omega_{PD}}{c}L_B\frac{n_H}{n_D}\frac{N_{10}^3}{(1+N_z^2)}, \tag{64}$$

which is in agreement with the result given by Francis *et al.*[14] in the limit $n_H/n_D \gg v_{Tb}^2/c_A^2$. This corresponds to the occurrence of a singularity in the wave equation. In contrast, the gyrokinetic theory yields a profile of finite width at the minority resonance, even when $N_z=0$.[3,4]

The perturbation result derived above is valid provided

$$r_2 \ll 4[r_1/(r_1-1)](k_z^2L_B^2+1)^{1/2}(\rho_b/L_B). \tag{65}$$

It can be seen that the perturbation analysis will be valid for larger minority to majority ratios when $k_zL_B \gg 1$. The condition for the validity of the perturbation analysis assumes that the fast wave is not near the fast wave cutoff. If this is not so, the condition is more stringent than Eq. (65).

We now return to the general dispersion relation given in Eq. (47). Substituting for Q, K_1, and K_2 from Eqs. (35)–(37), we write the dispersion relation in terms of $\mathbf{N}$:

$$(N_x^2+N_y^2)\left[1-(r_1^2-1)\left(\frac{r_2}{4r_1}-N_z^2+\frac{c_A^2}{c^2}\right)\right]$$
$$-\left\{1+\frac{r_2}{2r_1}\left(1+5r_1+\frac{3r_2}{r_1}(r_1^2-1)\right)-2\left(N_z^2-\frac{c_A^2}{c^2}\right)\left[1-\frac{(r_1^2-1)}{2}\left(\frac{r_2}{2r_1}-N_z^2+\frac{c_A^2}{c^2}\right)\right]\right\}$$
$$=\frac{r_2}{2r_1}(r_1^2-1)\frac{L_B}{\rho_b}\frac{1}{(k_z^2L_B^2+1)^{1/2}}\Bigg(Z(\eta_{1b})\Big\{(N_x+iN_y)(N_x-i\tau^2N_y)-\frac{[1+\tau^2-(v_{Tb}^2/2c_A^2)(N_x^2+N_y^2)]}{(r_1+1)}$$
$$\times\left[1+(r_1+1)\left(\frac{c_A^2}{c^2}+\frac{3}{2}\frac{r_2}{r_1}-N_z^2\right)\right]\Big\}+\nu\tau[1+\eta_{1b}Z(\eta_{1b})]\Big\{\left(N_y\frac{v_{Tb}}{c_A}(N_x-iN_y)-2i\nu\tau N_y\eta_{1b}\right)(N_x+iN_y)$$
$$-\frac{2}{(r_1+1)}\left[1+(r_1+1)\left(\frac{c_A^2}{c^2}+\frac{3}{2}\frac{r_2}{r_1}-N_z^2\right)\right]\left(i\frac{v_{Tb}}{c_A}N_x+\nu\tau\eta_{1b}\right)\Big\}\Bigg). \tag{66}$$

Using Eqs. (16), (17), and (22) we may write the quantity η_{1b} in the form

$$\eta_{1b} = -\frac{[x/\rho_b + (iN_x/2)(v_{Tb}/c_A)]}{(1+k_z^2L_B^2)^{1/2}}. \tag{67}$$

The dispersion relation, Eq. (66) has been solved numerically for N_x as a function of the normalized distance x/ρ_b. The equation is valid for any minority to majority density ratio and any value of k_z. The dispersion relation describes three-dimensional propagation since N_y is included in addition to N_x and N_z. The plasma conditions are specified through the parameters $r_1, r_2, v_{Tb}/c_A, c_A/c$, and L_B/ρ_b. We solve the dispersion relation as a function of x/ρ_b through the resonance region from large negative values of x/ρ_b to large positive values. The optical depth is then calculated by carrying out the numerical integration

$$\tau_b = 2\frac{\omega}{c_A}\int_{-\Delta}^{\Delta} \operatorname{Im} N_x\, dx, \tag{68}$$

where the upper and lower limits of integration $\pm\Delta$ are determined by observing the positions on either side of the resonance where $\operatorname{Im} N_x$ becomes negligible. This numerical procedure allows us to check the accuracy of the expansion used in Eqs. (57) and (58).

Our procedure for obtaining the optical depth is based on the self-consistent local dispersion relation. It is only expected to be reliable when either the minority dissipation is strong enough to remove the hybrid resonance and its associated cutoff or when the minority damping region is well separated from the hybrid resonance. When this is not the case a full wave theory is required. The extension of the present gyrokinetic analysis to the full wave case is left for a future publication. We shall give examples of the change observed in the solutions as the hybrid cutoff appears or is approached.

Let us now obtain an approximate condition for the occurrence of the hybrid resonance. Since we shall only present numerical solutions of Eq. (66) for the case $N_y = 0$, we will restrict the analysis to this case. There is no sharp transition from conditions when the hybrid resonance is present to those when it is not. However, a critical condition can be identified by the vanishing of the real part of the coefficient of N_x^2 in Eq. (66) with the constraint that $\operatorname{Re} Z(\eta_{1b})$ takes its maximum value.[12] For $N_y = 0$ this condition can be written

$$1 + (r_1^2 - 1)N_z^2 - \frac{r_2}{2r_1}(r_1^2-1)\frac{L_B}{\rho_b}\frac{1}{(k_z^2L_B^2+1)^{1/2}} \times \operatorname{Re} Z(\eta_{1b}) = 0. \tag{69}$$

For our purposes, we may approximate the maximum value of $\operatorname{Re} Z$ by unity and hence obtain a critical value of $r_2\,(=n_{0b}Z_b/n_{0a}Z_a)$ from Eq. (69),

$$(r_2)_{\text{crit}} \simeq [2r_1/(r_1^2-1)](\rho_b/L_B)(k_z^2L_B^2+1)^{1/2} \times [1 + (r_1^2-1)N_z^2]. \tag{70}$$

For values of r_2 significantly less than $(r_2)_{\text{crit}}$ the hybrid resonance will not occur, whereas for r_2 significantly larger, the resonance and its associated cutoff will be present.

Since the solution of Eq. (66) gives the variation through the resonance region, it is useful to employ this information to obtain the change in the electric field polarization. We therefore return to Eqs. (44) and (45) to obtain

$$\frac{\delta E_x \pm i\delta E_y}{\delta E_y} = \frac{\{k_y(k_x \pm ik_y) \pm i[k_z^2 - (\omega^2/c^2)] + 4\pi(\omega/c^2)(\pm\sigma_{xx} + i\sigma_{xy})\}}{[k_y^2 + k_z^2 - (\omega^2/c^2) - 4\pi i(\omega/c^2)\sigma_{xx}]}. \tag{71}$$

Substituting Eqs. (31), (32), and (38)–(40) into Eq. (71), we obtain

$$\frac{\delta E_x \pm i\delta E_y}{\delta E_y} = \left[k_y(k_x \pm ik_y) \pm i\left(k_z^2 - \frac{\omega^2}{c^2}\right) - i\frac{\omega}{c^2}\frac{\omega_{pa}^2}{\Omega_a}\left(\frac{r_1}{(r_1\pm 1)} + \frac{(5\pm 1)}{4}r_2 - \frac{r_2\omega}{k_z v_{Tb}}\frac{(1\mp 1)}{2}\tau K_1\right)\right]$$
$$\times\left[k_y^2 + k_z^2 - \frac{\omega^2}{c^2} + \frac{\omega^2}{c^2}\frac{\omega_{pa}^2}{\Omega_a}\left(\frac{r_1}{(r_1^2-1)} - \frac{r_2}{4} - \frac{r_2\omega}{2k_z v_{Tb}}\tau K_1\right)\right]^{-1}, \tag{72}$$

where we have put $\exp(-k_\perp^2\rho_b^2/4) \simeq 1$ in K_1 since $k_\perp^2\rho_b^2 \ll 1$. For $k_y = 0$, and using Eq. (36), we obtain

$$\frac{\delta E_x \pm i\delta E_y}{\delta E_y} = i\left[\pm\left(k_z^2 - \frac{\omega^2}{c^2}\right) - \frac{\omega}{c^2}\frac{\omega_{pa}^2}{\Omega_a}\left(\frac{r_1}{(r_1\pm 1)} + \frac{(5\pm 1)}{4}r_2 - r_2\frac{\omega}{k_z v_{Tb}}\frac{(1\mp 1)}{2}\tau Z(\eta_{1b})\right)\right]$$
$$\times\left[k_z^2 - \frac{\omega^2}{c^2} + \frac{\omega}{c^2}\frac{\omega_{pa}^2}{\Omega_a}\left(\frac{r_1}{(r_1^2-1)} - \frac{r_2}{4} - \frac{r_2\omega}{2k_z v_{Tb}}\tau Z(\eta_{1b})\right)\right]^{-1}. \tag{73}$$

IV. NUMERICAL SOLUTIONS OF THE LOCAL DISPERSION RELATION

In this section we present results obtained from a numerical solution of Eq. (66). These solutions enable us to treat any minority to majority density ratio, and to span the small region around $x = 0$ where the expansions used in Eqs. (57) and (58) break down. Our aim in these computations is to provide a simple and therefore fast method for calculating the transmitted power in a realistic magnetic field. Since the gyrokinetic model gives the self-consistent particle response, the field variation through the resonance region is also obtained. However, the calculations are only expected to be accurate under conditions where reflection is negligible. Reflection will occur when the two-ion hybrid resonance exists

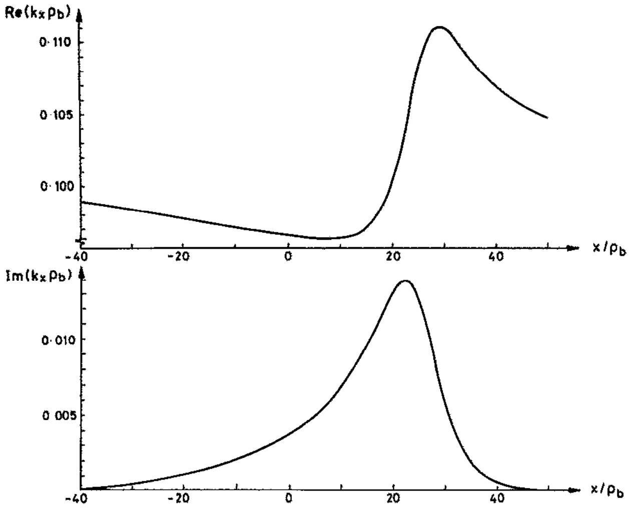

FIG. 1. An example of the regime where the two-ion hybrid resonance and cutoff are absent. Real (upper) and imaginary (lower) parts of $k_x\rho_b$ as a function of x/ρ_b for a D(^{3}He) plasma. Key dimensionless parameters are $r_2 = 10^{-2}$, $v_{Tb}/c_A = 0.1$, $k_z L_B = 20$, $L_B/\rho_b = 5\times 10^3$, and $c_A^2/c^2 = 3\times 10^{-5}$.

in the plasma. Thus, the condition given in Eq. (70) provides a marker for the applicability of our method. When reflection is significant the single-mode analysis used in this paper should be replaced by a full wave treatment based on the self-consistent local dispersion relation.

We illustrate this point in Figs. 1 and 2. Figure 1 shows a case where r_2 is less than the critical value. It can be seen that the real part of k_x varies by about 10% across the resonance region, but there is no cutoff. Figure 2 refers to a case where r_2 exceeds the critical value given in Eq. (70); the two-ion hybrid cutoff is present, and is well separated from the minority resonance region. In what follows, we shall only present results where the wave propagation has the character illustrated in Fig. 1, which occurs when the minority to majority density ratio is less than the critical value given in Eq. (70). Whenever the cutoff appears, we terminate the calculation.

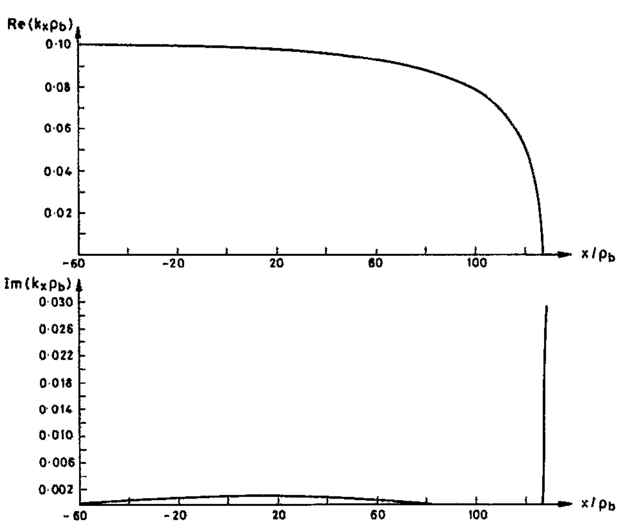

FIG. 2. An example of the regime where the minority ion cyclotron resonant damping region (at left) is well separated from the two-ion hybrid cutoff (at right). Real (upper) and imaginary (lower) parts of $k_x\rho_b$ as a function of x/ρ_b for a D(^{3}He) plasma. Key dimensionless parameters are $r_2 = 5\times 10^{-2}$, $v_{Tb}/c_A = 0.1$, $k_z L_B = 30$, $L_B/\rho_b = 10^4$, and $c_A^2/c^2 = 3\times 10^{-5}$.

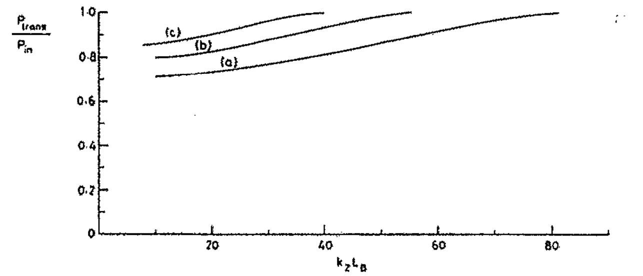

FIG. 3. The ratio of transmitted power to input power as a function of $k_z L_B$ for the regime illustrated in Fig. 1, where majority ion density n_{0a} = (a) $10^{20}\,\mathrm{m}^{-3}$, (b) $5\times 10^{19}\,\mathrm{m}^{-3}$, (c) $2.5\times 10^{19}\,\mathrm{m}^{-3}$. The plasma parameters are $n_{0b}/n_{0a} = 0.01$, $T_b = 2$ keV, $L_B/\rho_b = 1822$, $B_0 = 3.4$ T, and $L_B = 3$ m.

We choose parameters typical of JET discharges.[15] Figures 3 and 4 show the variation of the fast wave transmission coefficient as a function of the normalized parallel wave number $k_z L_B$, where L_B is equated with the major radius of JET which we have taken as 3 m. The magnetic field has been taken as 3.4 T and the temperature of the minority species as 2 keV. We assume a deuterium majority with a helium-3 minority in all computations. Figure 3 refers to a minority to majority density ratio of 1% [$r_2 = 0.02$, recalling the definition after Eq. (42)] and Fig. 4 to a ratio of 5% ($r_2 = 0.1$). In both figures, three curves are presented. Curve (a) refers to a deuterium density of $10^{20}\,\mathrm{m}^{-3}$, curve (b) to a deuterium density of $5\times 10^{19}\,\mathrm{m}^{-3}$, and curve (c) to a deuterium density of $2.5\times 10^{19}\,\mathrm{m}^{-3}$. As expected, the transmission decreases with the density. For 1% ^{3}He, the transmission at the highest density tends to a minimum close to 70%; for 5% ^{3}He, the lowest transmission is less than 20% at the highest density. The curves in Figs. 3 and 4 have all been terminated for the lower values of $k_z L_B$ due to the appearance of a cutoff. The lowest value of the transmission occurs for a value of r_2 close to the critical value given by Eq.

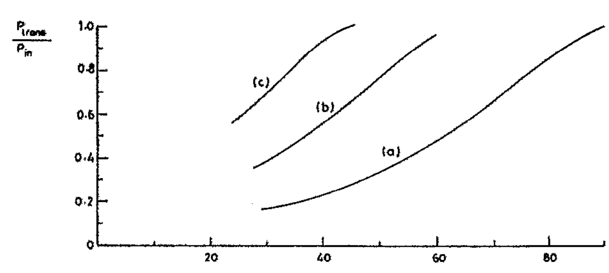

FIG. 4. The ratio of transmitted power to input power as a function of $k_z L_B$ for the regime illustrated in Fig. 1, where majority ion density n_{0a} = (a) $10^{20}\,\mathrm{m}^{-3}$, (b) $5\times 10^{19}\,\mathrm{m}^{-3}$, (c) $2.5\times 10^{19}\,\mathrm{m}^{-3}$. The plasma parameters are $n_{0b}/n_{0a} = 0.05$, $T_b = 2$ keV, $L_B/\rho_b = 1822$, $B_0 = 3.4$ T, and $L_B = 3$ m.

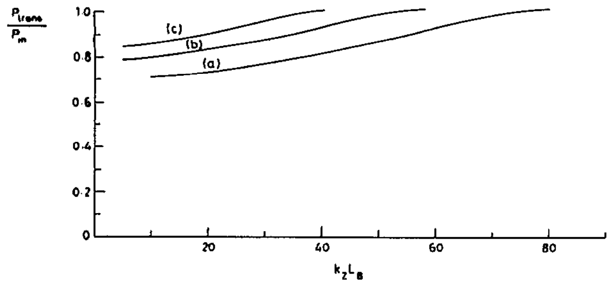

FIG. 5. The ratio of transmitted power to input power as a function of $k_z L_B$ for the regime illustrated in Fig. 1, where majority ion density n_{0a} = (a) $10^{20}\,\mathrm{m}^{-3}$, (b) $5\times10^{19}\,\mathrm{m}^{-3}$, (c) $2.5\times10^{19}\,\mathrm{m}^{-3}$. The plasma parameters are $n_{0b}/n_{0a} = 0.01$, $T_b = 8$ keV, $L_B/\rho_b = 911$, $B_0 = 3.4$ T, and $L_B = 3$ m.

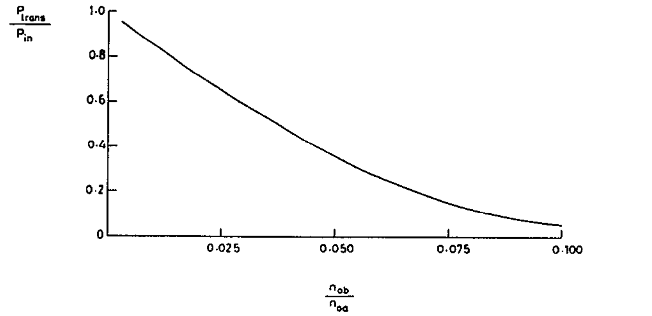

FIG. 7. The ratio of transmitted power to input power as a function of minority ion density, expressed as n_{0b}/n_{0a} for the case $n_{0a} = 5\times10^{19}\,\mathrm{m}^{-3}$. The plasma parameters are $T_b = 8$ keV, $L_B/\rho_b = 911$, $k_z L_B = 30$, $B_0 = 3.4$ T, and $L_B = 3$ m.

(70). In order to complete the curves in Figs. 3 and 4, a full wave theory would be required for the lower values of $k_z L_B$.

Figures 5 and 6 refer to the same parameters as Figs. 3 and 4, except for the minority temperature which is now 8 keV. The curves are effectively identical to those for 2 keV, except that the curves for 8 keV extend to lower values of $k_z L_B$ before the cutoff intervenes. This is to be expected; it reflects the fact that the optical depth is independent of minority ion temperature, as was noted in our perturbation analysis at Eq. (61). The dependence of the transmission coefficient on the minority to majority density ratio is shown in Fig. 7. This curve was obtained for a fixed value of $k_z L_B = 30$, for a deuterium density of $5\times10^{19}\,\mathrm{m}^{-3}$ and for a minority temperature of 8 keV. The transmission coefficient falls to a value of 5% for a 10% minority to majority ratio. The curve has been terminated for $r_2 = 0.2$ due to the occurrence of the cutoff for larger values of r_2. Again note that the lowest transmission occurs under conditions which are close to the appearance in the plasma of the hybrid resonance. The transition from a resonance free situation, shown in Fig. 1, to one where the hybrid resonance occurs is indicated by a progressive sharpening of the variation of the real and imaginary parts of k_x through the absorption region. The transmission curve as a function of r_2 possesses a rather flat minimum. The minority to majority density ratio for which this minimum occurs is given to within a factor of 2 by the formula for $(r_2)_{\rm crit}$ in Eq. (70).

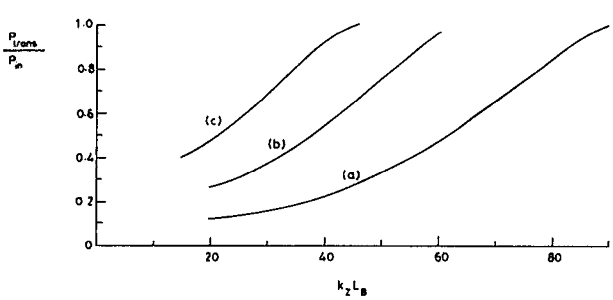

FIG. 6. The ratio of transmitted power to input power as a function of $k_z L_B$ for the regime illustrated in Fig. 1, where majority ion density n_{0a} = (a) $10^{20}\,\mathrm{m}^{-3}$, (b) $5\times10^{19}\,\mathrm{m}^{-3}$, (c) $2.5\times10^{19}\,\mathrm{m}^{-3}$. The plasma parameters are $n_{0b}/n_{0a} = 0.05$, $T_b = 8$ keV, $L_B/\rho_b = 911$, $B_0 = 3.4$ T, and $L_B = 3$ m.

We conclude this section by presenting some results concerning the perpendicular absorption mechanism arising from the inclusion in the gyrokinetic analysis of the variation of the magnetic field across the minority ion Larmor radius.[3,4] For perpendicular propagation, the optical depth is given by Eq. (62). For $k_z L_B = 0$, $L_B/\rho_b = 1191$, and again considering D(^{3}He) for which $r_1 = 4/3$, Eq. (70) gives the critical value $(r_2)_{\rm crit} \simeq 0.003$. This value satisfies the criterion for the perturbation formula to be valid and gives an optical depth of 3.5%. This agrees with the value obtained from a solution of the general dispersion relation, Eq. (66). To investigate much larger values of r_2 (minority to majority density ratios) we must solve Eq. (66) numerically. Increasing r_2 to a value of 0.1 and obtaining the optical depth from Eq. (66), we now find a value of only 0.4%. Thus, by increasing the minority to majority ratio by a factor of 30, the fast wave loses almost no energy in crossing the minority resonance.

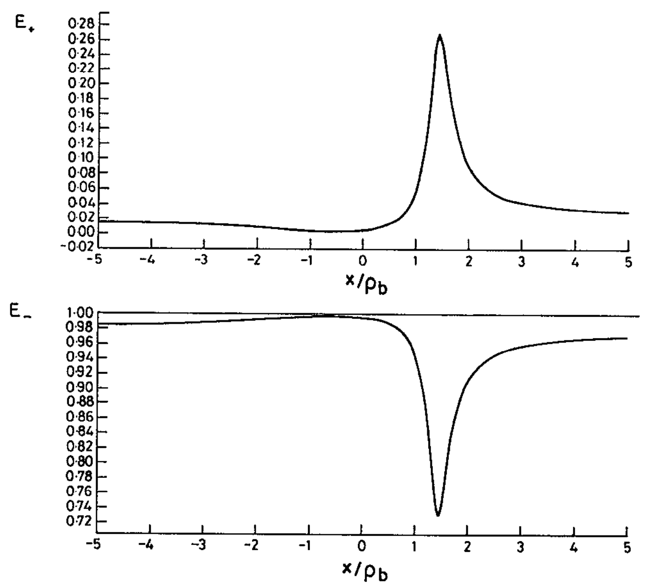

FIG. 8. Magnitude of left circularly polarized wave field E_+ (upper) and right circularly polarized wave field E_- (lower) as a function of x/ρ_b for a case where the two-ion hybrid resonance is absent. The plasma parameters are $n_{0b}/n_{0a} = 0.0015$, $n_{0a} = 5\times10^{19}\,\mathrm{m}^{-3}$, $T_b = 5$ keV, $L_B/\rho_b = 1191$, $k_z L_B = 0$, $B_0 = 3.4$ T, and $L_B = 3.1$ m.

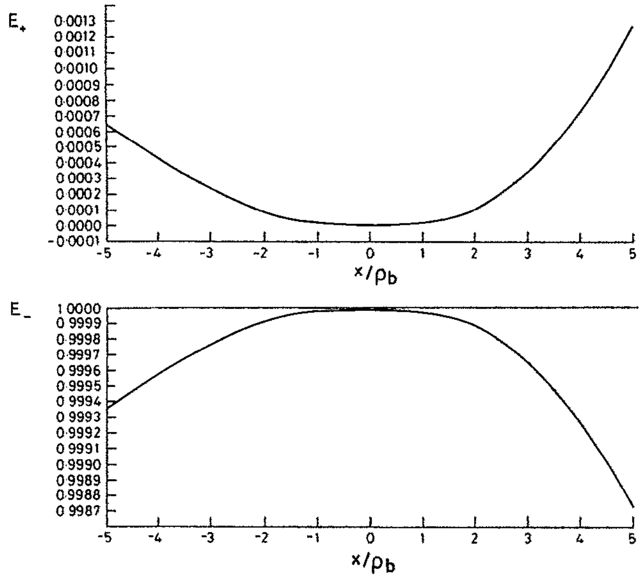

FIG. 9. Magnitude of left circularly polarized wave field E_+ (upper) and right circularly polarized wave field E_- (lower) as a function of x/ρ_b for a case where the two-ion hybrid resonance is present. Here $n_{0b}/n_{0a} = 0.05$ and other plasma parameters are as for Fig. 8.

The explanation for this behavior can be found in the change in the electric field polarization as a function of r_2. Figures 8 and 9 show the variation of the two field polarizations

$$E_+ = (\delta E_x + i\delta E_y)/(|\delta E_x|^2 + |\delta E_y|^2)^{1/2}$$

and

$$E_- = (\delta E_x - i\delta E_y)/(|\delta E_x|^2 + |\delta E_y|^2)^{1/2}$$

across the minority resonance region, obtained from Eq. (73) for two different cases. Figure 8 refers to the case $r_2 = 0.003$ and shows that the E_+ component, which is responsible for the resonant interaction with the minority ions, is almost zero except close to the resonance where it is enhanced to about 26%. On the other hand, for $r_2 = 0.1$, Fig. 9 shows the opposite behavior. Again, E_+ is very small outside the resonance region, but in the resonance region, it is depressed to even lower values, consistent with almost 100% transmission.

The behavior just described suggests the following interpretation of the perpendicular damping mechanism. For small values of $r_2 \lesssim (r_2)_{\rm crit}$, the hybrid resonance is either overlapped by the minority resonance or does not occur. Even when the hybrid resonance does not exist, there is still an associated variation of the real part of the wave number which enhances the field polarization in the region where absorption can occur. Thus, the condition to maximize the perpendicular absorption is that the minority to majority density ratio should correspond to $(r_2)_{\rm crit}$. Substituting the value for $(r_2)_{\rm crit}$ into Eq. (62) for $\tau_{b\perp}$, we obtain

$$(\tau_{b\perp})_{\max} \simeq \pi(v_{Tb}/c_A)[(r_1 - 1)/(r_1 + 1)]. \qquad (74)$$

For a given plasma species, this suggests that the optical depth for perpendicular propagation depends on the single dimensionless parameter v_{Tb}/c_A, independent of the machine scale length L_B, but now dependent on the minority temperature.

We have used Eq. (66) to test the scaling given by Eq. (74) for minority temperatures ranging from 5 to 200 keV for JET parameters. Taking the deuterium density to be $5\times 10^{19}\,{\rm m}^{-3}$, $B_0 = 3.4$ T, and $L_B = 3.1$ m, we first calculate the values of $(r_2)_{\rm crit}$ for various minority temperatures: see Table I, which also lists the quantity v_{Tb}/c_A. Since $k_x\rho_b \simeq v_{Tb}/c_A$, it is clear that $k_x^2\rho_b^2 \ll 1$ for the minority temperatures chosen. The dispersion relation Eq. (66) is now solved for the above parameters, giving the results shown in Table II. These were obtained by starting with a low value of r_2 which was then gradually increased until a cutoff appeared. The optical depth is given for the value of r_2 just below that at which the cutoff appears; this is to be compared with the corresponding quantity predicted by Eq. (74) and given by the fourth column of Table I. The value of r_2 just before the cutoff appears is also given for comparison with $(r_2)_{\rm crit}$. Once the cutoff appears, a full wave theory should be used. The results obtained from Eq. (66) are given in Table II. Comparing Tables I and II we see that the general behavior is borne out. The optical depth increases linearly with v_{Tb}/c_A at first, but falls off a little for larger values of v_{Tb}/c_A. The value of r_2 agrees to within a factor of 2 with $(r_2)_{\rm crit}$.

TABLE I. Values of $(r_2)_{\rm crit}$ from Eq. (70) and $(\tau_{b\perp})_{\max}$ from Eq. (74), for increasing values of minority ion temperature T_b. Deuterium density $n_{0a} = 5\times 10^{19}\,{\rm m}^{-3}$, $B_0 = 3.4$ T, and $L_B = 3.1$ m.

T_b (keV)	v_{Tb}/c_A	L_B/ρ_b	$(r_2)_{\rm crit}$	$(\tau_{b\perp})_{\max}$
5	0.0762	1191.0	0.0029	0.034
10	0.108	842.6	0.0041	0.049
20	0.152	595.8	0.0058	0.068
50	0.241	376.8	0.0091	0.11
100	0.341	266.6	0.013	0.15
200	0.482	188.4	0.018	0.22

TABLE II. Values of r_2 just below cutoff and of τ, obtained from Eq. (66), for increasing values of minority ion temperature T_b. Bulk plasma parameters are the same as Table I.

T_b (keV)	v_{Tb}/c_A	L_B/ρ_b	r_2	τ
5	0.0762	1191.0	0.003	0.036
20	0.152	595.8	0.005	0.060
100	0.341	266.6	0.009	0.12
200	0.482	188.4	0.0095	0.14

TABLE III. Values of r_2 just below cutoff and of τ, obtained from Eq. (66), for increasing values of minority ion temperature T_b. Deuterium density $n_{0a} = 2\times 10^{20}\,{\rm m}^{-3}$, $B_0 = 3.4$ T, and $L_B = 3.1$ m.

T_b (keV)	v_{Tb}/c_A	L_B/ρ_b	r_2	τ
5	0.152	1191.0	0.003	0.070
20	0.304	595.8	0.0042	0.11
50	0.482	376.8	0.005	0.15

TABLE IV. Values of r_2 just below cutoff and of τ, obtained from Eq. (66), for increasing values of magnetic inhomogeneity length scale L_B. Minority ion temperature $T_b = 10$ keV and deuterium density $n_{0a} = 2\times10^{20}$ m^{-3}.

L_B(m)	v_{Tb}/c_A	L_B/ρ_b	r_2	$(r_2)_{crit}$	τ
1.03	0.216	280.9	0.011	0.012	0.091
3.1	0.216	842.6	0.0036	0.0041	0.087
6.2	0.216	1685.0	0.0018	0.0020	0.087

A similar comparison is made in Table III, which was obtained from Eq. (66) for a higher deuterium density, $n_{0a} = 2\times10^{20}$ m^{-3}. The scaling is similar to the previous results: the optical depth increases with v_{Tb}/c_A, and r_2 is within a factor of 2 of $(r_2)_{crit}$.

In Table IV we demonstrate the effect of changing L_B while keeping the density and temperature fixed. Table IV supports the conjecture that the maximum optical depth for perpendicular propagation is independent of the scale length. The value obtained is in good agreement with Eq. (74), which gives 0.097; r_2 and $(r_2)_{crit}$ are closer for this case.

The results presented in Tables I–IV lend support to the conjecture that the perpendicular damping depends only on the parameter v_{Tb}/c_A. Thus, for strong perpendicular absorption, high ion temperatures are required such that $v_{Tb} > c_A$. This is the regime of the fusion products and also of minority tails in present discharges with ion cyclotron resonant heating (ICRH). In order to extend the analysis to this regime, we must generalize the present treatment to include $k_\perp\rho_i > 1$, since $k_\perp\rho_i \simeq v_{Ti}/c_A$. We also note that the optical depth for the minority ion resonance in this high ion temperature regime is evidently proportional to the minority temperature; this is in contrast to the standard result.

V. CONCLUSIONS

In this paper we have extended the gyrokinetic theory of cyclotron resonance to include propagation at arbitrary angles to the equilibrium magnetic field. Our aim in the present work has been to provide a more accurate and yet simpler means for calculating the transmission coefficient for fast wave heating in the ion cyclotron range of frequencies. The increase in accuracy stems from the capability of gyrokinetic theory to include the self-consistent particle response in a nonuniform magnetic field. The simplicity of our approach is due to our use of a single-mode treatment based on the self-consistent local dispersion relation. This dispersion relation is valid for arbitrary ratios of the minority to majority density. However, when this ratio exceeds the critical value defined in Sec. III, the present single-mode treatment is no longer valid and a full wave theory is required. Such a calculation will be presented in the near future.

The single-mode description that we have employed is most reliable when either the minority absorption region is well separated from the hybrid resonance or the minority cyclotron damping is strong enough to remove the hybrid resonance. We have estimated a critical minority to majority density ratio, below which the hybrid resonance is expected to be absent. Most of the results we have presented have been obtained for this condition. The dependence of the transmission coefficient on the minority to majority ratio, the minority temperature, and the majority density as a function of $k_z L_B$ has been presented.

The analysis given in this paper is three dimensional since it contains the three components of the wave vector: k_x, k_y, and k_z. For simplicity, we have restricted our numerical examples to the $k_y = 0$ case. Since the gyrokinetic theory automatically includes the kinetic power flow,[3,4] we are able to calculate the variation of the electric field polarization through the resonance region.

We have also presented further results on the perpendicular ion cyclotron damping mechanism previously identified.[3–5] It has been found that this damping is only significant below a certain minority to majority density ratio which is proportional to ρ_b/L_B. For minority densities below this value, the hybrid resonance does not occur and perpendicular damping takes place. For minority densities larger than the critical value, the hybrid resonance occurs with the result that the right circularly polarized component of the electric field is reduced almost to zero in the minority resonance region and there is no damping. When the occurrence of the hybrid resonance removes the damping in the vicinity of the minority resonance, the fast wave interacts strongly with the plasma around the hybrid resonance, where mode conversion to an ion Bernstein wave takes place. This is beyond the scope of the present single-mode analysis. Our results suggest that the perpendicular damping is proportional to v_{Tb}/c_A. Strong perpendicular damping is therefore expected when $v_{Tb} \geqslant c_A$, which corresponds to $k_\perp\rho_b \geqslant 1$. In order to investigate this regime, relevant to fusion products and ICRH-generated ion tails, the present analysis must be extended to include $k_\perp\rho_b \gtrsim 1$.

ACKNOWLEDGMENT

We are extremely grateful to Terry Martin for his expert coding of the general dispersion relation.

[1] L. Chen and S. T. Tsai, Phys. Fluids **26**, 141 (1983).
[2] L. Chen and S. T. Tsai, Plasma Phys. **25**, 349 (1983).
[3] C. N. Lashmore-Davies and R. O. Dendy, Phys. Rev. Lett. **62**, 1982 (1989).
[4] C. N. Lashmore-Davies and R. O. Dendy, Phys. Fluids B **1**, 1565 (1989).
[5] X. S. Lee, J. R. Myra, and P. J. Catto, Phys. Fluids **26**, 223 (1983).
[6] K. Imre, H. Weitzner, and D. B. Batchelor, in *Applications of Radio Frequency Power in Plasmas*, AIP Conf. Proc. 159, edited by S. Bernabei and R. W. Motley (American Institute of Physics, New York, 1986), p. 358.
[7] D. J. Gambier and A. Samain, Nucl. Fusion **25**, 283 (1985).
[8] H. A. Romero and G. J. Morales, Phys. Fluids B **1**, 1805 (1989).
[9] H. Ye and A. N. Kaufman, Phys. Rev. Lett. **61**, 2762 (1988).
[10] H. Ye and A. N. Kaufman, in *Radio Frequency Power in Plasmas*, AIP Conf. Proc. 190, edited by R. McWilliams (American Institute of Physics, New York, 1989), p. 374.
[11] R. A. Cairns, C. N. Lashmore-Davies, R. O. Dendy, B. M. Harvey, R. J. Hastie, and H. Holt, Phys. Fluids B **3**, 2953 (1991).
[12] C. N. Lashmore-Davies, V. Fuchs, G. Francis, A. K. Ram, A. Bers, and L. Gauthier, Phys. Fluids **31**, 1614 (1988).
[13] N. A. Krall and A. W. Trivelpiece, *Principles of Plasma Physics* (McGraw-Hill, New York, 1973), p. 405.
[14] G. Francis, A. Bers, and A. K Ram, in Ref. 6, p. 370.
[15] J. Jacquinot and the JET Team, Plasma Phys. **30**, 1467 (1988).